BNL 37502

CONF-8510265--1

LOW ENERGY $P\bar{P}$ STRONG INTERACTIONS: THEORETICAL PERSPECTIVE*

Carl B. Dover

Brookhaven National Laboratory**
Upton, New York 11973

BNL--37502

DE86 005810

*Invited talk at the Workshop on the Design of a Low Energy Antimatter Facility in the USA, Madison, Wisconsin; October 3-5, 1985.

REFERENCES

1. W. W. Buck, C. B. Dover and J. M. Richard, Ann. Phys. (NY) 121, 47 (1979); C. B. Dover and J. M. Richard, Ann. Phys. (NY) 121, 70 (1979).
2. C. B. Dover and J. M. Richard, Phys. Rev. C21, 1466 (1980).
3. J. Coté et al, Phys. Rev. Lett. 48, 1319 (1982).
4. P. H. Timmers, W. A. van der Sanden and J. J. deSwart, Phys. Rev. D29, 1928 (1984).
5. R. Bertini et al, "Measurement of Spin Dependent Observables in the $\bar{p}N$ Elastic Scattering from 300 MeV/c to 700 MeV/c," LEAR proposal (October 1985).
6. A. M. Green and J. A. Niskanen, Intern. Rev. of Nucl. Phys., Vol. II, ed. T. T. S. Kuo (World Scientific Co., Singapore, 1984); Nucl. Phys. A412, 448 (1984) and A431, 593 (1984).
7. M. Maruyama and T. Ueda, Nucl. Phys. A364, 297 (1981); M. Maruyama, Prog. Theor, Phys. 69, 937 (1984) and Thesis (Osaka University, 1984).
8. M. Kohno and W. Weise, Phys. Lett. 152B, 303 (1985); R. Tegen, T. Mizutani and F. Myhrer, preprint (1985).
9. S. Furui, A. Faessler and S. B. Khadkikar, Nucl. Phys. A424, 495 (1984); S. Furui, Orsay preprints (1985); C. B. Dover and P. M. Fishbane, Nucl. Phys. B244, 349 (1984).
10. C. B. Dover, "Quark Dynamics of $N\bar{N}$ Annihilation," Proc. of the Intern. Symposium on Medium Energy Nucleon and Antinucleon Scattering, Bad Honnef, Germany, to be published by Springer Verlag, Berlin.
11. C. B. Dover and J. M. Richard, Phys. Rev. C25, 1952 (1982).
12. N. Hoshizaki, Suppl. Prog. Theor. Phys. 42, 107 (1968).
13. C. L. Csonka, Nucl. Inst. and Meth. 63, 247 (1968); K. Kilian and D. Möhl, Proc. LEAR Workshop, Erice, 1982, p. 701; E. Steffens, Proc. LEAR Workshop, Tignes, France, January 1985.
14. B. Moussallam, These de Doctorat D'Etat, Université Pierre et Marie Curie, Paris, France (May 1985).
15. J. K. Storrow, Phys. Rep. 103, 317 (1984).
16. B. Moussallam, Nucl. Phys. A407, 413 (1983) and A429, 429 (1984).
17. R. Armenteros and B. French, in "High Energy Physics," ed. E. H. S. Burhop, Academic Press, New York (1969), p. 293.
18. S. Ahmad et al, "$p\bar{p}$ Annihilation at Rest from Atomic P States," Proc. of the LEAR Workshop, Tignes, France (1985).
19. J. A. Niskanen and F. Myhrer, Phys. Lett. 157B, 247 (1985)
20. A. Le Yaouanc, L. Oliver, O. Pène and J. C. Raynal, Phys. Rev. D8, 2223 (1973).
21. N. Isgur and J. Paton, Oxford preprint (1985).
22. C. B. Dover, P. M. Fishbane and S. Furui, manuscript in preparation.
23. C. B. Dover, J. M. Richard and M. Zabek, Ann. Phys. (NY) 130, 70 (1980).
24. S. Ahmad et al, "$p\bar{p}$ Annihilation into Neutral Kaons," CERN/EP 85-53 (1985).

LOW ENERGY $P\bar{P}$ STRONG INTERACTIONS: THEORETICAL PERSPECTIVE

Carl B. Dover

Brookhaven National Laboratory*
Upton, New York 11973

ABSTRACT

Several of the frontier problems in low energy nucleon-antinucleon phenomenology are addressed. Spin observables and dynamical selection rules in $N\bar{N}$ annihilation are used as examples of phenomena which offer particularly strong constraints on theoretical models, formulated either in terms of meson and baryon exchange or as effective operators in a non-perturbative quark-gluon picture.

INTRODUCTION

The problem of nucleon-antinucleon ($N\bar{N}$) interactions is a fascinating one. In the low and medium energy (0 - 2 GeV/c) regime, the advent of the LEAR (Low Energy Antiproton Ring) facility at CERN has led to a renaissance of interest in a whole class of fundamental questions related to the physics of the $N\bar{N}$ system. Several of these questions are discussed in these Proceedings, for instance the tests of fundamental symmetries, the search for baryonium and other exotic mesons, etc. Here, we restrict our attention to the three following problems:

i) How can we construct quantitative theoretical models for the low energy $N\bar{N}$ interaction?

ii) To what extent can we understand the low energy $N\bar{N}$ data in terms of conventional meson and baryon exchange mechanisms?

iii) Which aspects of the $N\bar{N}$ problem, if any, require the explicit introduction of the underlying quark-gluon degrees of freedom?

In trying to answer i), we will review the implications of the G-parity rule, which relates the meson exchange contributions to the real part of the NN and $N\bar{N}$ potentials. Questions ii) and iii) are intimately related to the process of $N\bar{N}$ annihilation. Even at rest, the $N\bar{N}$ system can dissolve into a sizable number of mesonic final states. The relative branching ratios for these states, if known precisely, exercise a strong constraint on the theory. We will discuss some recent data on $p\bar{p} \to \pi^+\pi^-\pi^0$ from LEAR, which indicate that dynamical selection rules operate in $N\bar{N}$ annihilation. It is argued that such rules are a signature of the underlying quark-gluon dynamics of the short range annihilation process. Other constraints on the theory are provided by the spin observables for the $p\bar{p} \to p\bar{p}$, $p\bar{p} \to n\bar{n}$ and $\bar{n}p \to \bar{n}p$ reactions. Much more than total cross sections, these observables probe the coherent tensor forces predicted by meson theory, and the spin-isospin dependence of the annihilation potential. We provide several examples of how future experiments at a

*supported under contract DE-AC02-76CH00016 with the U. S. Department of Energy.

high intensity low energy $\bar{p}$ facility, with a capability for polarized beams and targets, would shed light on a variety of fundamental questions.

RELATION BETWEEN NN AND $N\bar{N}$ INTERACTIONS

The connection between the meson exchange contribution to the NN and $N\bar{N}$ potentials (real, non-annihilation part) is provided by the G-parity rule. Given an interaction potential

$$V_{NN} = \sum_i V_i \tag{1}$$

for the nucleon-nucleon (NN) system, where i labels the contribution of any meson exchange ($i = \{\pi, \eta, \rho, \omega, \delta, \varepsilon \cdots\}$), the corresponding potential $V_{N\bar{N}}$ is given by

$$V_{N\bar{N}} = \sum_i G_i V_i \ , \tag{2}$$

where G_i is the G-parity of meson i. In coordinate space, the potentials V_i have the form

$$V_i = \left(\begin{matrix}1\\ \tau_1\cdot\tau_2\end{matrix}\right) \cdot \left(V_0^i + V_\sigma^i\, \sigma_1\cdot\sigma_2 + V_{LS}^i\, L\cdot S + V_T^i S_{12} + V_{LS2} Q_{12}\right) \tag{3}$$

corresponding to isoscalar (1) or isovector ($\tau_1 \cdot \tau_2$) exchanges. The tensor and quadratic spin orbit operators S_{12} and Q_{12} have the well known form

$$\begin{aligned} S_{12} &= 3\sigma_1\cdot\hat{r}\ \ \sigma_2\cdot\hat{r} \ - \ \sigma_1\cdot\sigma_2 \\ Q_{12} &= 1/2\ (\sigma_1\cdot L\ \sigma_2\cdot L + \sigma_2\cdot L\ \sigma_1\cdot L) \end{aligned} \tag{4}$$

where L is the relative orbital angular momentum and $S = (\sigma_1 + \sigma_2)/2$ is the total intrinsic spin.

The apparently innocent phase factor $G_i = \pm 1$ produces an $N\bar{N}$ potential which is qualitatively different from that for the NN case. The key concept[1] is coherence, namely the tendency for all mesons i to yield a contribution of the same sign to certain components of the interaction. For the NN system, scalar (ε) and vector (ω) meson exchange add coherently in the spin orbit term V_{LS}, while they tend to cancel in the central part V_0. Pseudoscalar (π) and vector (ρ) contributions appear with like signs in V_σ and opposite signs in V_T. The coherent spin-orbit potential is evident in NN scattering, for instance, the zero in the $^3P_0$ phase shift is due to the short range coherent and repulsive V_{LS} (which gives $\delta<0$) competing against the long range attraction arising from π exchange (which alone leads to $\delta>0$).

For $N\bar{N}$, in contrast, coherences occur in the central ($\omega+\varepsilon$), tensor ($\pi+\rho$) and quadratic spin-orbit potentials. The very strong $N\bar{N}$ attraction due to V_0 leads one to predict a number of bound states[1], most of which are expected to be very broad and difficult to observe. The coherent tensor force for $N\bar{N}$ has several striking consequences for spin observables, which we discuss later. To summarize, although

both the NN and $N\bar{N}$ real potentials arise from the same set of meson exchange potentials V_i , the different linear combinations

$$\sum_i V_i \text{ and } \sum_i G_i V_i$$

of Eqs. (1) and (2) emphasize complementary aspects of the same underlying exchange mechanism.

THE $N\bar{N}$ ANNIHILATION POTENTIAL

Since the $N\bar{N}$ system has zero baryon number, it can dissolve into a spray of mesons, an option not available to the NN system. In the language of the optical model, these processes can be simulated by a means of a complex annihilation potential $V_{ann}(r)$. There are several recent attempts[2,3,4] to account for the available $N\bar{N}$ cross section data in terms of a semi-phenomenological optical potential consisting of a theoretical meson exchange part $\sum_i G_i V_i$ supplemented by a parametrized form for $V_{ann}(r)$. In ref.[2], a spin, isospin and energy independent Woods-Saxon function was assumed:

$$V_{ann}(r) = -(V_0 + iW_0)/(1 + e^{(r-R)/a}) \quad . \tag{5}$$

Two parameter choices which can account for the data on total $N\bar{N}$ elastic, charge exchange and annihilation cross sections are given by Dover and Richard[2], namely

$$\begin{aligned} &R = 0, \quad a = 1/5\text{fm}, \; V_0 = 21 \text{ GeV}, \; W_0 = 20 \text{ GeV} \quad \text{(Model DR I)} \\ &R = 0.8\text{fm}, \; a = 1/5\text{fm}, \; V_0 = 500 \text{ MeV}, \; W_0 = 500 \text{ MeV} \quad \text{(Model DR II)} \end{aligned} \tag{6}$$

The Paris group[3] analyzed all the available $N\bar{N}$ data, including angular distributions, assuming Re $V_{ann} = 0$, but with a more flexible form for the absorptive potential:

$$\text{Im } V_{ann}(r) = \left\{ g_c(1+f_c E) + g_{ss}(1+f_{ss}E)\, \sigma_1\cdot\sigma_2 + g_T S_{12} + \frac{g_{LS}}{4m^2} L\cdot S \frac{1}{r}\frac{d}{dr} \right\} \frac{K_0(2mr)}{r} \quad . \tag{7}$$

The range parameter 1/2m was held fixed at 0.1 fm (nucleon exchange) and the numerous other parameters (different for isospin I = 0,1) were adjusted to produce a best fit. The resulting model will be referred to as "PARIS." Models DR I, DR II and PARIS use very similar versions of the meson exchange part $\sum_i G_i V_i$ of the $N\bar{N}$ potential.

The PARIS model[3] is characterized by a marked dependence of $V_{ann}(r)$ on spin, isospin and energy. The spin dependence is particularly strong: the absorption for spin S=0 is roughly an order of magnitude larger than for S=1. The isospin dependence is milder although still significant. This model stands in sharp contrast to that of the Nijmegen group[4], who use a coupled channel framework, with coupling potentials dependent on I but not on S.

Clearly the existing $N\bar{N}$ data are insufficient to uniquely determine the spin-isospin dependence of $V_{ann}(r)$, since only a limited amount of elastic polarization information exists, and the other spin observables remain completely unmeasured. One of the potentialities

of LEAR is that this void in the $\bar{N}N$ data could be at least partially filled in. Recently, Bertini et al[5] have presented a clever proposal for a measurement of several $\bar{p}N$ spin observables, using a thin polarized target and measuring the spin state of the recoiling nucleon. This experiment counts on the increased antiproton intensity which will be available during the ACOL era of LEAR.

In the discussion which follows, we compare the predictions of the DR I, DR II and PARIS models for spin observables. These models have the virtue of retaining quantitative contact with the data, and the disadvantage of having essentially no theoretical input as to the form of V_{ann} (except for the choice of $K_0(2mr)/r$ in Eq. (7), which corresponds to a nucleon exchange picture of annihilation).

Recently, there has been a surge of interest in trying to derive V_{ann} in terms of a quark-gluon picture. This approach might be referred to as "applied quantum chromodynamics" at low energy, in a regime where perturbative QCD does not apply. The Helsinki[6] and Osaka[7] groups have made extensive studies of quark rearrangement and annihilation models for $N\bar{N}$ annihilation, with semi-quantitative success in explaining mesonic branching ratios and $N\bar{N}$ scattering data. There is much recent work on the problem of which effective operator to use for a quark-antiquark ($Q\bar{Q}$) annihilation vertex, i.e., an operator with the quantum numbers of one gluon[8], or alternatively, those of the vacuum (the $^3P_0$ model[9]). A critical discussion of these alternatives can be found in ref. (10). The potential V_{ann} which results from the quark models[6-10] is dependent on S, I, and E; Im V_{ann} increases with E, as found in ref. (3), but the spin dependence is not particularly strong. Thus there appears to be no justification in the framework of the quark model for an S=0 absorptive potential which is an order of magnitude stronger than for S=1, as found in the PARIS model[3]. Unfortunately, no predictions of spin observables have yet been worked out in quark-gluon models of the $N\bar{N}$ interaction. As these models become more quantitative, this will be an important task.

SPIN OBSERVABLES

Since $N\bar{N}$ forces depend strongly on spin and isospin in a complicated way, they cannot be deduced uniquely from a few measurements such as the differential cross section and polarization. In general, difficult experiments involving polarized beams and/or polarized targets are required. This places a premium on obtaining high intensity $\bar{N}$ beams. Some of the relevant experiments will be possible[5] in the ACOL era of LEAR. Note that the determination of the isospin dependence of the $N\bar{N}$ force involves a study of charge exchange ($p\bar{p}\to n\bar{n}$) and $\bar{n}p$ (or equivalently $\bar{p}n$) elastic scattering in addition to the $p\bar{p}\to p\bar{p}$ channel. Since charge exchange cross sections are small, the measurement of spin quantities will be even more demanding than for $p\bar{p} \to p\bar{p}$. However, the most dramatic spin effects are expected in $p\bar{p} \to n\bar{n}$, as we see later. One might try to obtain information on $\bar{p}n$ scattering by studying $\bar{p}d$ in the spectator regime, or by using charge exchange to produce a polarized $\bar{n}$ beam and then scattering it from a hydrogen target.

In this section, we present a variety of predictions for spin observables in $N\bar{N}$ scattering, using the models DR I, DR II, and PARIS developed earlier. We emphasize the interplay between the coherent tensor force and the spin-isospin dependence of the annihilation potential. The results displayed here supplement those given in ref. (11). We use the notation of Hoshizaki[12], who discussed the formalism for the case of NN scattering. The structure of the formulae is essentially the same for NN and $N\bar{N}$, except that the symmetries due to the Pauli principle are absent for $N\bar{N}$ ($\theta \to \pi - \theta$ relations, restrictions of I and S).

Tensor forces play a dominant role in $N\bar{N}$ spin physics, but their effect is already evident in total cross sections, particularly that for charge exchange, as shown in Fig. 1. If we start with the exact PARIS model, and turn off various spin dependent components of the NN interaction (both real and imaginary parts) in turn, we see that the tensor (S_{12}) component is most important. The $p\bar{p} \to n\bar{n}$ cross section σ_{CE} drops by a factor of three if tensor forces are set to zero! In σ_{CE}, the coherent contribution of $\pi + \rho$ exchange enters, although the pion plays the most important role because of its long range.

The same strong tensor force effect is visible in many of the spin observables. For example, the depolarization D as a function of $\cos\theta$ (θ = lab scattering angle) is shown in Fig. 2 at a lab kinetic energy E = 130 MeV. If S_{12} and Q_{12} terms are turned off, D is practically unity, its value in the absence of any spin dependence. With tensor forces, D differs dramatically from 1 in the backward hemisphere. The angular dependence of D is very different for elastic scattering and charge exchange. The sharp structure in D for small angles is almost model independent, and reflects the dominant one pion exchange contribution.

The depolarization D is accompanied by the spin rotation parameters R, A, R' and A', which occur on the same footing. Let $\vec{p}_i$ and $\vec{p}_f$ be the incident and outgoing $\bar{N}$ momenta in the lab system, and choose an orthogonal set of unit vectors

$$\begin{aligned} \hat{n} &= \vec{p}_i \times \vec{p}_f / \left|\vec{p}_i \times \vec{p}_f\right| \\ \hat{s}_i &= \hat{n} \times \hat{p}_i \\ \hat{p}_i &= \vec{p}_i / \left|\vec{p}_i\right| \end{aligned} \tag{8}$$

for the initial state i and another set $\{\hat{n}, \hat{s}_f, \hat{p}_f\}$ for the final state f. Now consider an incident $\bar{N}$ beam prepared with polarization $\langle\sigma\rangle_i$, while the target nucleon is assumed to be unpolarized. Then the differential cross section is given by

$$d\sigma/d\Omega = \left(d\sigma/d\Omega\right)_{\text{unpol}} + \frac{1}{4}\langle\vec{\sigma}\rangle_i \cdot \mathrm{Tr}(M\vec{\sigma}M^{+}) \tag{9}$$

where M is the $N\bar{N}$ scattering amplitude, normalized so that the cross section $\left(d\sigma/d\Omega\right)_{\text{unpol}}$ for an unpolarized $\bar{N}$ incident on an unpolarized N is $\mathrm{Tr}\left(MM^{+}\right)/4$. The lab expectation value $\langle\vec{\sigma}\rangle_f$ of the $\bar{N}$ spin in the final state is given by

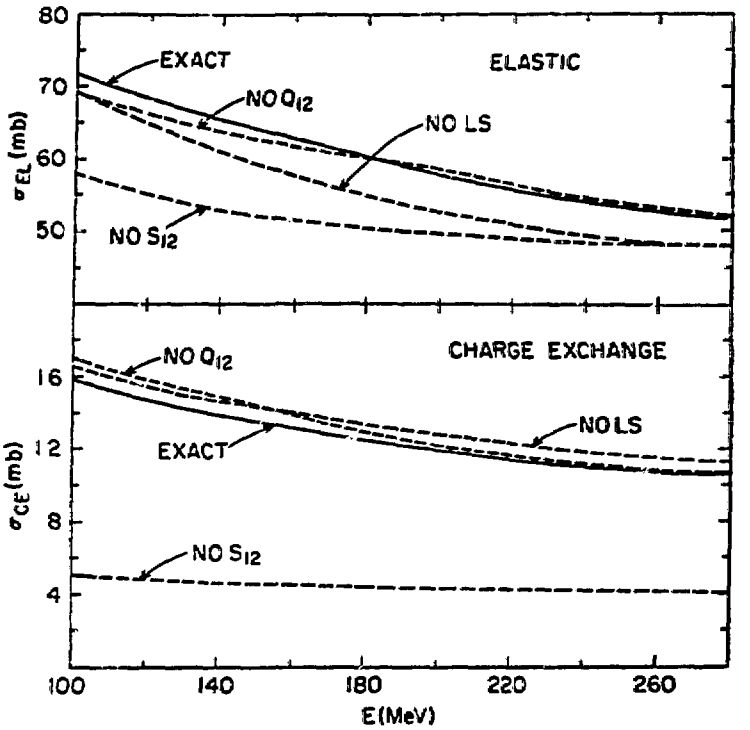

Fig. 1. Total $p\bar{p} \to p\bar{p}$ elastic and $p\bar{p} \to n\bar{n}$ charge exchange cross sections σ_{EL} and σ_{CE} as a function of lab kinetic energy E. The solid curves represent the results obtained using the full PARIS $N\bar{N}$ optical potential. The dashed curves show the effect of turning off one spin dependent component (both real and imaginary parts) at a time. LS, Q_{12}, and S_{12} refer to the spin-orbit, quadratic spin-orbit and tensor components, respectively, of the potential.

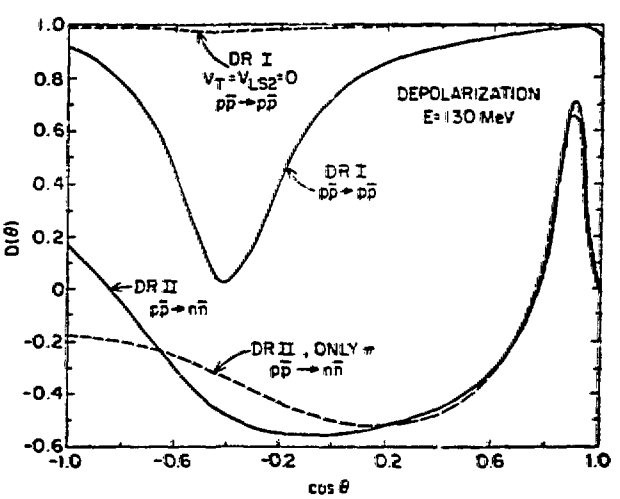

Fig. 2. The depolarization parameter D as a function of the cosine of the lab scattering angle θ, at E = 130 MeV.

$$\langle \vec{\sigma} \rangle_f \frac{d\sigma/d\Omega}{(d\sigma/d\Omega)_{unpol}} = (P + D\langle\sigma_n\rangle_i)\hat{n} + (A\langle\sigma_{p_i}\rangle_i + R\langle\sigma_{s_i}\rangle_i)\hat{s}_f + (A'\langle\sigma_{p_i}\rangle_i + R'\langle\sigma_{s_i}\rangle_i)\hat{p}_f \ . \quad (10)$$

Now consider some special cases. For an $\bar{N}$ beam with unit polarization along $\hat{n}$, we find

$$\langle\sigma_n\rangle_f = \frac{D + P}{1 + P} \ . \quad (11)$$

Thus if D=1, the scattered beam remains completely polarized along $\hat{n}$. In general, we have $|\langle\sigma_n\rangle_f| \leq 1$, so that $2|P| - 1 \leq D \leq 1$. Suppose now that we prepare the $\bar{N}$ beam with polarization +1 along $\hat{s}_i$ (transverse to the beam direction). Then

$$\begin{aligned} \langle\sigma_n\rangle_f &= P \\ \langle\sigma_{s_f}\rangle_f &= R \\ \langle\sigma_{p_f}\rangle_f &= R' \end{aligned} \quad (12)$$

or, equivalently,

$$\begin{aligned} R &= (1-P^2)^{1/2} \cos(\theta-\beta) \\ R' &= (1-P^2)^{1/2} \sin(\theta-\beta) \end{aligned} \quad (13)$$

where θ is the lab scattering angle and β is the angle of rotation of the $\bar{N}$ polarization vector in the scattering plane. A and A' have a similar interpretation to R and R' for a case where the incident $\bar{N}$ has unit polarization along $\hat{p}_i$ (longitudinal).

In Figs. 3 and 4, we display predictions of $d\sigma/d\Omega$, P, D, R, A, R', A' for elastic $p\bar{p} \to p\bar{p}$ scattering for lab kinetic energies of E = 160 and 220 MeV. Models DR I and PARIS are seen to yield very similar predictions for the elastic scattering angular distribution, since only the spin-averaged optical potential is involved here. The spin observables show a more marked model dependence, with the PARIS results showing more dramatic angular structures. The sharpest angular variation in D, R, A, R' and A' occurs in the region of the diffraction minimum in $d\sigma/d\Omega$. Here, where we are best able to distinguish the theoretical models, the cross sections are small (typically 0.1 - 0.2 mb/sr) and the experimental measurements will be most difficult. In the forward angle region ($\cos\theta \geq 0.6$), $d\sigma/d\Omega$ is about two orders of magnitude larger, but the model dependence of the spin observables is much more modest, so precision measurements will be needed. In any case, the study of $N\bar{N}$ spin physics, although rewarding, appears difficult, and certainly requires the highest possible $\bar{p}$ intensities.

The main features of the $N\bar{N}$ potential, as mentioned earlier, are a strong isospin dependent tensor component and an annihilation part W, which could depend strongly on spin, isospin, and energy. The interplay between these components, as reflected in the spin observables, is very complicated. Measurements of the full angular dependence of spin quantities at several energies are necessary in order to attempt to disentangle the energy-independent tensor term coming from t-channel meson exchange from spin and energy dependent contributions

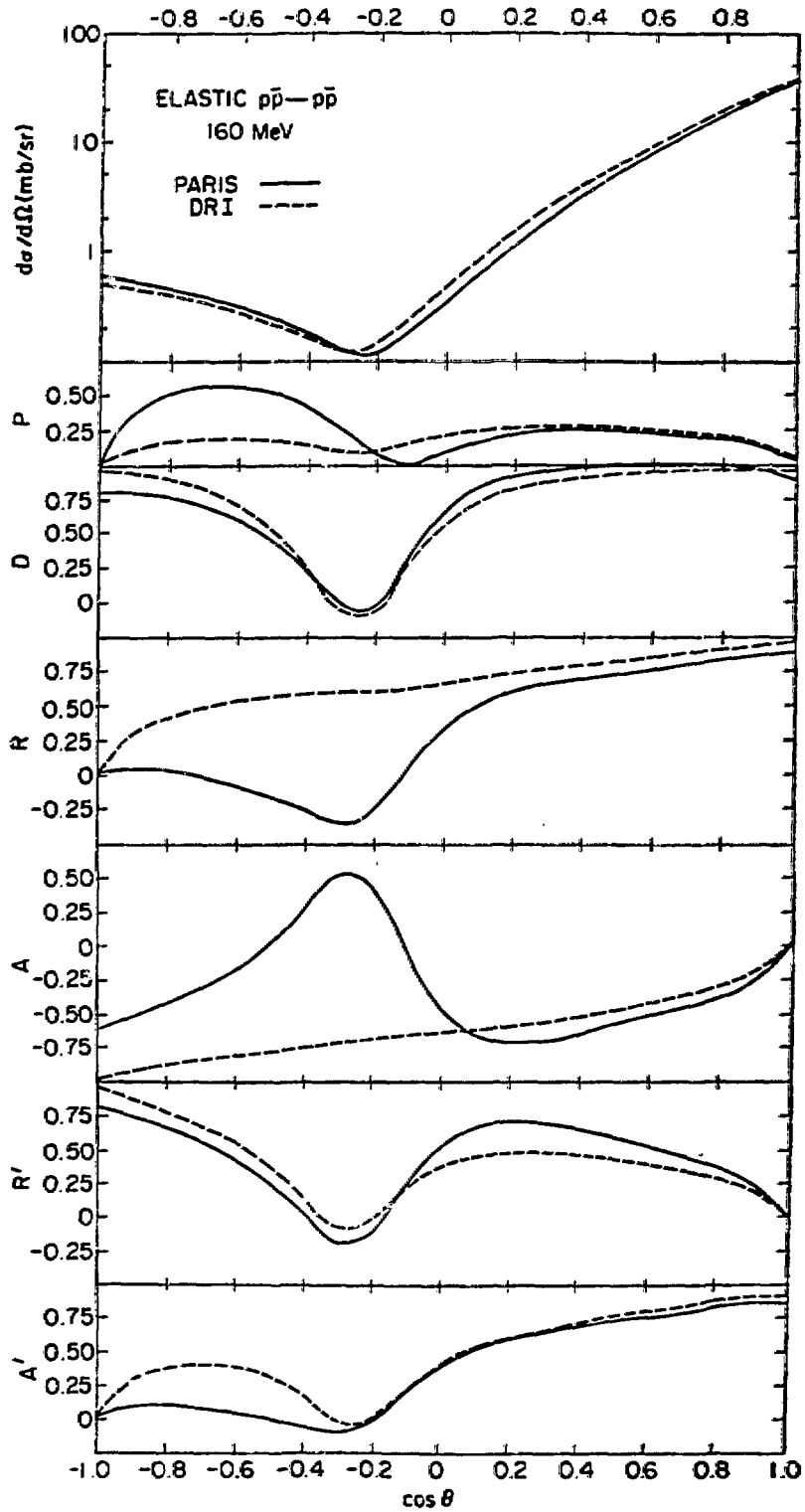

Fig. 3. Differential cross section $d\sigma/d\Omega$ and spin observables P, R, A, R', A' for elastic $p\bar{p}$ scattering at E = 160 MeV. The predictions for the PARIS and DR I models are shown as solid and dashed lines.

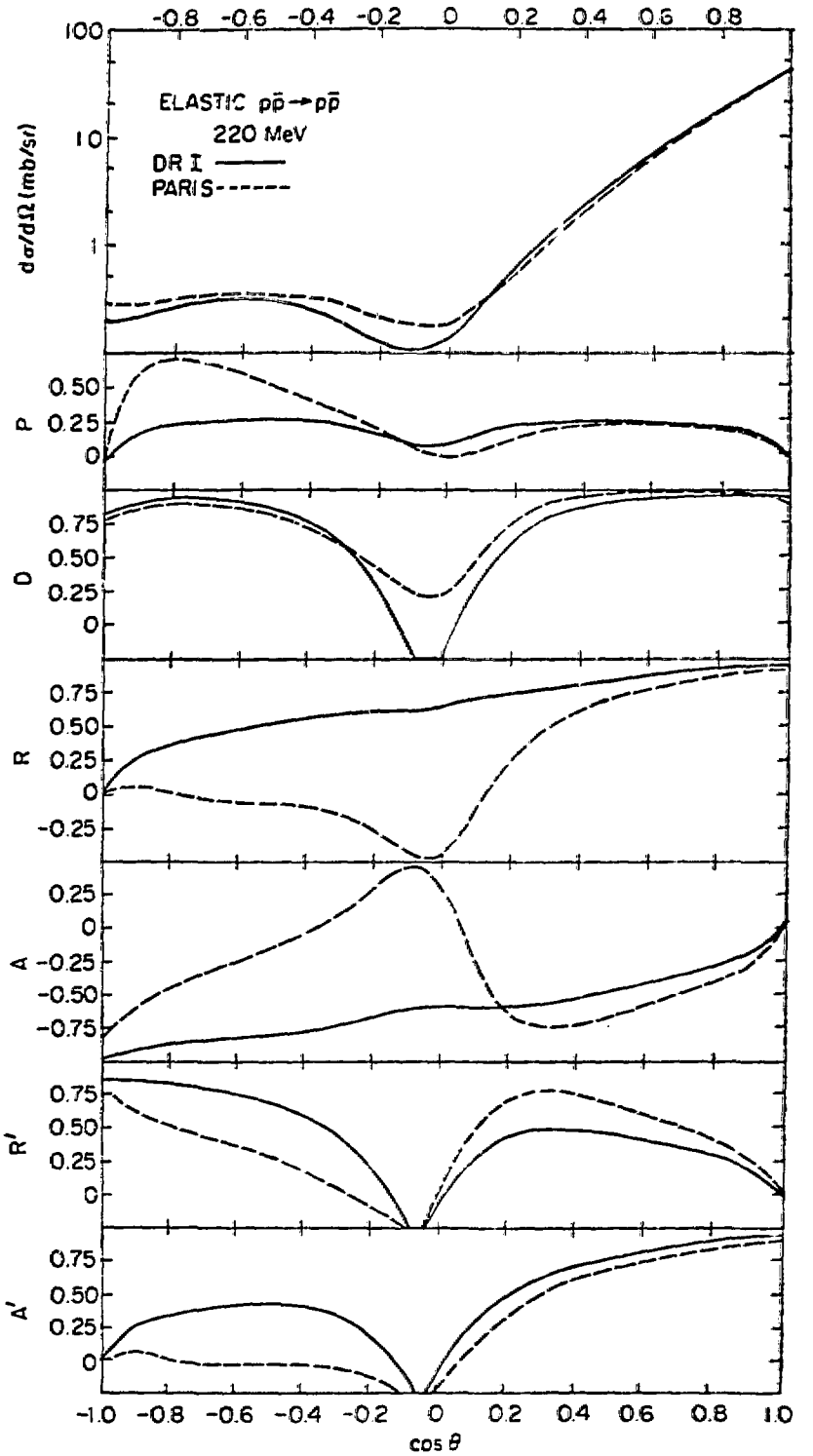

Fig. 4. Same as Fig. 3 for E = 220 MeV (PARIS results now appear as dashed lines).

coming from annihilation (i.e., s-channel meson exchange).

In Figs. 5 and 6, we show the energy dependence of D, R, A, R' and A' for model DR I. The sharp minima in D, R' and A' track the movement of the diffraction minimum in $d\sigma/d\Omega$. The observables R and A are predicted to be only weakly dependent on energy in model DR I. In the PARIS model, on the other hand, the energy dependence is more pronounced.

The strong spin dependence of W in the PARIS model is evident in the differences

$$\Delta\sigma_L = \sigma_{\overrightarrow{\leftarrow}} - \sigma_{\overrightarrow{\rightarrow}}$$
$$\Delta\sigma_T = \sigma_{\downarrow\uparrow} - \sigma_{\uparrow\uparrow} \qquad (14)$$

of cross sections for different longitudinal (L) or transverse (T) spin orientations with respect to the direction defined by the incident $\bar{N}$ beam momentum. The ratios $\Delta\sigma_{L,T}/\sigma$, where σ is the appropriate spin-averaged cross section, are shown for elastic (EL), charge exchange (CE) and annihilation (A) cross sections in Figs. 7, 8, and 9. For models DR I and DR II, the deviations of $\Delta\sigma/\sigma$ from zero primarily reflect the influence of the coherent tensor potential (here W is spin independent). For elastic scattering, the effect of the strong spin dependence of W in the PARIS model is to more than double the values of $\Delta\sigma_L/\sigma$ and $\Delta\sigma_T/\sigma$ (for $E > 150$ meV).

As seen in Fig. 8, the spin effects are particularly dramatic for $p\bar{p} \to n\bar{n}$ charge exchange. $(\Delta\sigma_L/\sigma)_{CE}$ is of order -1 throughout the low energy regime, i.e., $\sigma_{\overrightarrow{\rightarrow}} \approx 3\sigma_{\overrightarrow{\leftarrow}}$. Again, the largest single effect is that of the tensor potential, which favors $N\bar{N}$ scattering in spin-aligned configurations. For example, we have

$$\Delta\sigma_T/\sigma = \begin{cases} -0.43 \text{ (exact)} \\ -0.38 \text{ (no } Q_{12}) \\ -0.35 \text{ (no LS)} \\ -0.11 \text{ (no } S_{12}) \end{cases} \qquad (15)$$

for $p\bar{p} \to n\bar{n}$ at E = 70 MeV in the PARIS model, and

$$\Delta\sigma_L/\sigma = \begin{cases} -0.72 \text{ (exact)} \\ -0.77 \text{ (no } Q_{12}) \\ -0.90 \text{ (no LS)} \\ -0.49 \text{ (no } S_{12}) \end{cases} \qquad (16)$$

From Eqs. (15) and (16), we see that the predicted spin dependence of $p\bar{p} \to n\bar{n}$ cross sections is considerably reduced if tensor (S_{12}) terms are suppressed, while the effect is much less dramatic if LS or Q_{12} terms are set to zero. Note that for $\Delta\sigma_L/\sigma$, however, there remains considerable spin dependence when tensor forces are absent (note that $\Delta\sigma_L/\sigma = -1/2$ implies $\sigma_{\overrightarrow{\rightarrow}} = 5/3\ \sigma_{\overrightarrow{\leftarrow}}$). For the PARIS model, this is mainly due to the strong spin dependence of W. Since the absorption into mesonic channels is much less strong for S=1 than for S=0 states in the PARIS model, the charge exchange cross section for S=1 will be larger than for S=0, i.e., $\sigma_{\overrightarrow{\rightarrow}}$, which corresponds to pure S=1, will exceed $\sigma_{\overrightarrow{\leftarrow}}$, which is a mixture of S=0, 1. Tensor forces augment this effect, since they produce additional attraction for S=1, while they are absent for S = 0.

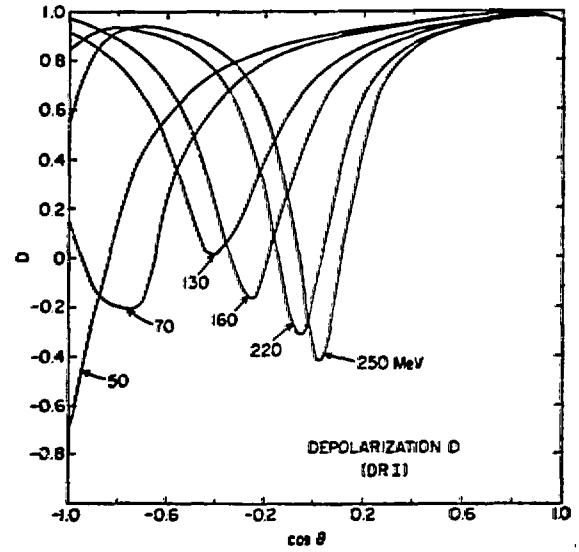

Fig. 5. Angular distributions for the depolarization D in model DR I at various lab energies from 50 to 250 MeV.

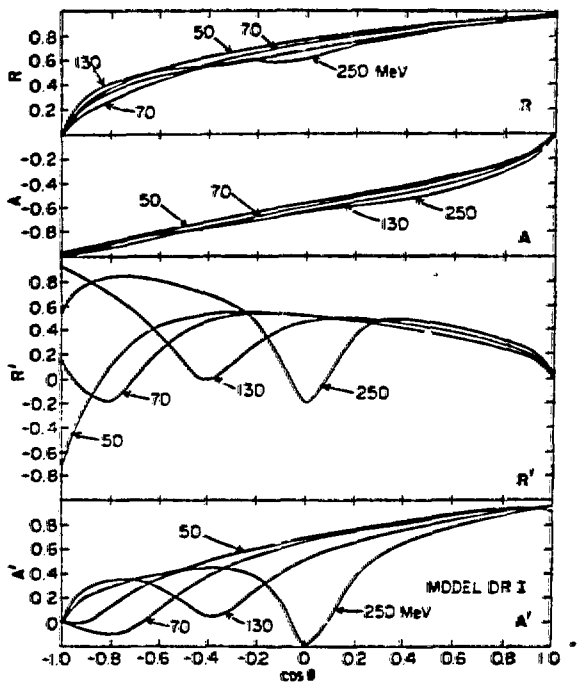

Fig. 6. Angular distributions for R, A, R' and A' in model DR I for E = 50, 70, 130 and 250 MeV.

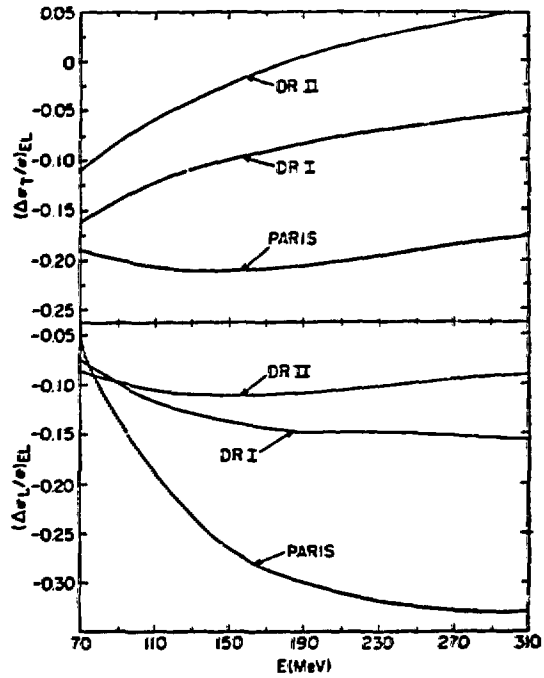

Fig. 7. The ratios $\Delta\sigma_T/\sigma$ and $\Delta\sigma_L/\sigma$ for $p\bar{p}$ elastic scattering as a function of E, for models DR I, DR II and PARIS for the $N\bar{N}$ potential.

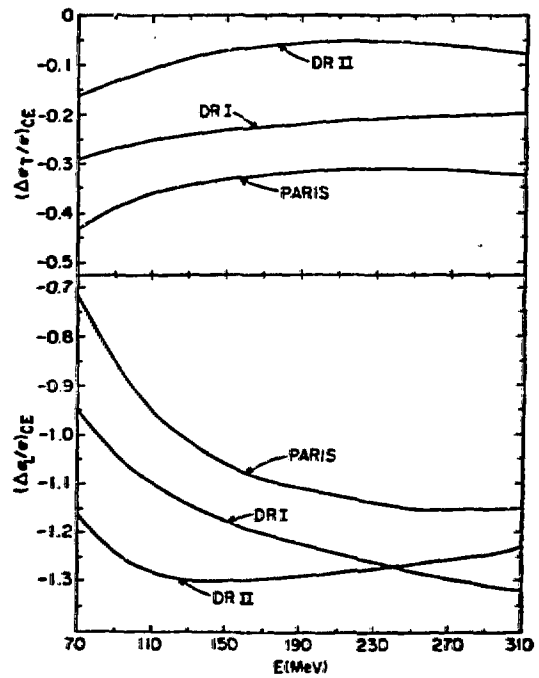

Fig. 8. Same as Fig. 7, but for $p\bar{p} \to n\bar{n}$ charge exchange.

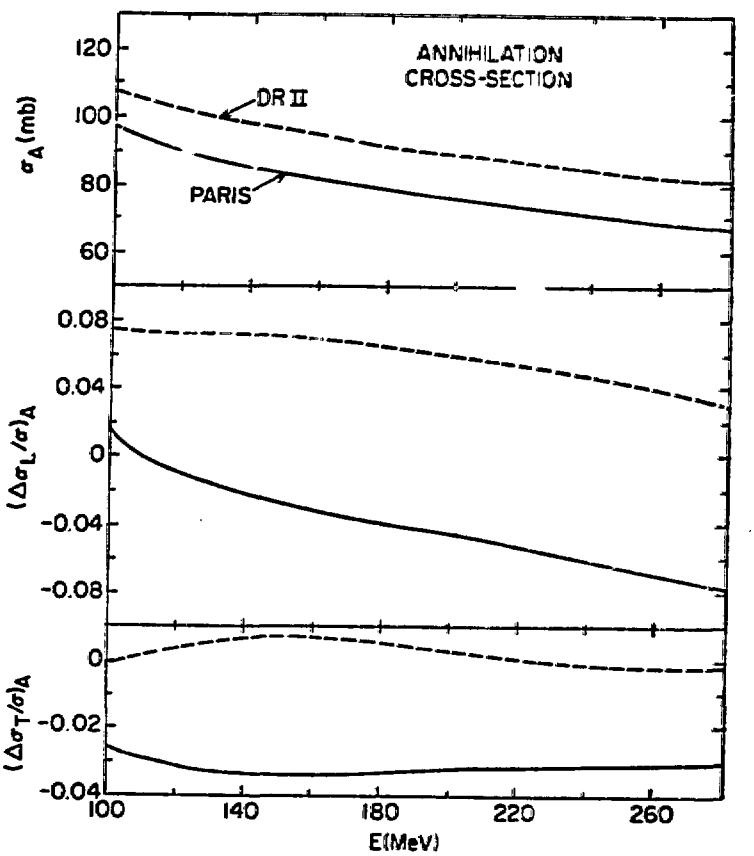

Fig. 9. Total $p\bar{p}$ cross section σ_A and the ratios $(\Delta\sigma_L/\sigma)_A$ and $(\Delta\sigma_T/\sigma)_A$ for annihilation as a function of E. PARIS and DR II predictions are shown as solid and dashed lines, respectively.

Other striking spin effects for $p\bar{p} \to n\bar{n}$ include the following[11]:

$$\begin{aligned} D(180°) &\approx -0.75 \\ A'(0°) &\approx -0.85 \\ A_t'(0°) &\approx +0.9 \end{aligned} \qquad (17)$$

for model DR I at E = 130 MeV. These strong effects persist at other energies in the other models. Even with an unpolarized $\bar{p}$ beam incident on an unpolarized target, the $p\bar{p} \to n\bar{n}$ reaction produces strongly polarized $\bar{n}$'s.

Although $\Delta\sigma_L/\sigma$ and $\Delta\sigma_T/\sigma$ are large for $p\bar{p} \to n\bar{n}$, they are rather small for the total annihilation cross section, as shown in Fig. 9. Although W depends strongly on spin, being stronger for S=0 in the PARIS model, the real potential, which is more attractive for S=1, has a compensating effect. For S=1, the increased attraction serves to focus the $N\bar{N}$ wave function to short distances, where absorption becomes more effective. The ratio $\sigma_A(S=0)/\sigma_A(S=1)$ thus does not simply follow the ratio $W_0(S=0)/W_0(S=1)$ of absorptive well depths. A similar effect is observed[14] for the widths of atomic levels of the $p\bar{p}$ system, i.e., $\Gamma(S=0)/\Gamma(S=1) \approx 2$ for the PARIS model, whereas $W_0(S=0)/W_0(S=1) \approx 10$.

The fact that $(\Delta\sigma_T/\sigma)_A$ is rather small, as per Fig. 9, implies that $(\Delta\sigma_T/\sigma)_{TOT}$ is also modest in size, since annihilation represents roughly 2/3 of the cross section. This has important implications for the spin filtering technique, which has been suggested[13] as a means of producing polarized $\bar{p}$ beams. The idea is to let an initially unpolarized $\bar{p}$ beam impinge on a polarized ($\uparrow$) hydrogen target. At time t = 0, the beam, of total intensity I_0, consists half of $\bar{p}(\uparrow)$ and half of $\bar{p}(\downarrow)$. Letting $\sigma_+ \equiv \sigma_{\uparrow\uparrow}^{TOT}$ and $\sigma_- \equiv \sigma_{\uparrow\downarrow}^{TOT}$, we find that the intensities $I_\pm$ of the $\bar{p}(\uparrow)$ and $\bar{p}(\downarrow)$ components of the beam are attenuated according to

$$\frac{dI_\pm}{dt} = -\sigma_\pm nf\, I_\pm = -(\sigma_0 \pm \sigma_1)nf\, I_\pm \qquad (18)$$

where n is the polarized target density, and f is the revolution frequency of the $\bar{p}$ beam. The total beam intensity $I(t) = I_+ + I_-$ at time t is given by

$$I(t) = I_0\, e^{-t/t_0} \cosh(t/t_1) \qquad (19)$$

while the polarization P(t) of the $\bar{p}$ beam, resulting from the inequality of σ_+ and σ_-, is

$$P(t) = (I_+ - I_-)/(I_+ + I_-) = -\tanh(t/t_1)\,, \qquad (20)$$

with $t_0 = 1/\sigma_0 nf$ and $t_1 = 1/\sigma_1 nf$. Now we note that

$$t_0/t_1 = \sigma_1/\sigma_0 = -1/2(\Delta\sigma_T/\sigma)_{TOT}\,. \qquad (21)$$

For $t < \frac{1}{2} t_1$, we have to a good approximation,

$$\begin{aligned} I(t) &\approx I_0\, e^{-t/t_0} \\ P(t) &\approx -t/t_1 \end{aligned} \qquad (22)$$

Thus t_0 is the time scale associated with the attenuation of the $\bar{p}$ beam intensity, and t_1 is the time needed to build up an appreciable $\bar{p}$ polarization.

If t_1 is comparable to t_0, we have a chance to produce polarized $\bar{p}$'s before the beam disappears due to interactions with the target. However, in a realistic case, as shown in Table I, we have $\sigma_1/\sigma_0 < 0.1$ in the whole low energy region for models DR I, DR II, and PARIS. Thus $t_1 > 10\ t_0$, and the situation is unfavorable for producing appreciable polarization. The most favorable case we have found is model DR I at energies $E < 50$ MeV. Here σ_1/σ_0 is somewhat larger than the values listed in Table 1. For instance, for $E = 30$ MeV, an energy considered by Steffens[13], we find $\sigma_{TOT} = 272$ mb, $\sigma_1/\sigma_0 = 0.075$. Using the values[13] $n = 10^{14}/cm^2$, $f = 10^6/sec$, we find

$$\begin{aligned} t_0 &= 10.2 \text{ hrs} \\ t_1 &= 13.3\ t_0 = 136 \text{ hrs} \ . \end{aligned} \tag{23}$$

At $t = 48$ hrs, we then find

$$\begin{aligned} I(t) &= 0.0096\ I_0 \\ P(t) &= -\ 0.34 \ . \end{aligned} \tag{24}$$

The prospects for the success of the spin filtering technique[13] are thus rather grim. Even using the maximum value of σ_1/σ_0 predicted by

TABLE I.

Cross Section Ratio σ_1/σ_0 for Spin Filtering

E (MeV)	σ_1/σ_0 (PARIS)	σ_1/σ_0 (DR I)	σ_1/σ_0 (DR II)
70	0.055	0.052	0.030
100	0.062	0.044	0.017
130	0.065	0.037	0.009
160	0.065	0.032	0.003
190	0.063	0.028	0.002
220	0.061	0.025	-0.002
250	0.060	0.022	-0.003
280	0.058	0.020	-0.004
310	0.056	0.018	-0.006

our models, we still lose 99% of the beam before the $\bar{p}$ polarization has built up to values of about $-1/3$. The assumption that $\sigma_1/\sigma_0 \geq 0.1$, used by Steffens[13], is more optimistic than our realistic models suggest.

The spin observables of low and medium energy $N\bar{N}$ scattering represent a sensitive test of our theories of the meson exchange and annihilation potentials. A number of dramatic spin effects are anticipated, particularly in the $p\bar{p} \to n\bar{n}$ channel. A variety of models

Other striking spin effects for $p\bar{p} \to n\bar{n}$ include the following[11]:

$$\begin{aligned} D(180°) &\approx -0.75 \\ A'(0°) &\approx -0.85 \\ A_C'(0°) &\approx +0.9 \end{aligned} \tag{17}$$

for model DR I at E = 130 MeV. These strong effects persist at other energies in the other models. Even with an unpolarized $\bar{p}$ beam incident on an unpolarized target, the $p\bar{p} \to n\bar{n}$ reaction produces strongly polarized $\bar{n}$'s.

Although $\Delta\sigma_L/\sigma$ and $\Delta\sigma_T/\sigma$ are large for $p\bar{p} \to n\bar{n}$, they are rather small for the total annihilation cross section, as shown in Fig. 9. Although W depends strongly on spin, being stronger for S=0 in the PARIS model, the real potential, which is more attractive for S=1, has a compensating effect. For S=1, the increased attraction serves to focus the $N\bar{N}$ wave function to short distances, where absorption becomes more effective. The ratio $\sigma_A(S=0)/\sigma_A(S=1)$ thus does not simply follow the ratio $W_0(S=0)/W_0(S=1)$ of absorptive well depths. A similar effect is observed[14] for the widths of atomic levels of the $p\bar{p}$ system, i.e., $\Gamma(S=0)/\Gamma(S=1) \approx 2$ for the PARIS model, whereas $W_0(S=0)/W_0(S=1) \approx 10$.

The fact that $(\Delta\sigma_T/\sigma)_A$ is rather small, as per Fig. 9, implies that $(\Delta\sigma_T/\sigma)_{TOT}$ is also modest in size, since annihilation represents roughly 2/3 of the cross section. This has important implications for the spin filtering technique, which has been suggested[13] as a means of producing polarized $\bar{p}$ beams. The idea is to let an initially unpolarized $\bar{p}$ beam impinge on a polarized ($\uparrow$) hydrogen target. At time t = 0, the beam, of total intensity I_0, consists half of $\bar{p}(\uparrow)$ and half of $\bar{p}(\downarrow)$. Letting $\sigma_+ \equiv \sigma^{TOT}_{\uparrow\uparrow}$ and $\sigma_- \equiv \sigma^{TOT}_{\downarrow\uparrow}$, we find that the intensities $I_\pm$ of the $\bar{p}(\uparrow)$ and $\bar{p}(\downarrow)$ components of the beam are attenuated according to

$$\frac{dI_\pm}{dt} = -\sigma_\pm nf\, I_\pm = -(\sigma_0 \pm \sigma_1)nf\, I_\pm \tag{18}$$

where n is the polarized target density, and f is the revolution frequency of the $\bar{p}$ beam. The total beam intensity $I(t) = I_+ + I_-$ at time t is given by

$$I(t) = I_0\, e^{-t/t_0} \cosh(t/t_1) \tag{19}$$

while the polarization P(t) of the $\bar{p}$ beam, resulting from the inequality of σ_+ and σ_-, is

$$P(t) = (I_+ - I_-)/(I_+ + I_-) = -\tanh(t/t_1)\ , \tag{20}$$

with $t_0 = 1/\sigma_0 nf$ and $t_1 = 1/\sigma_1 nf$. Now we note that

$$t_0/t_1 = \sigma_1/\sigma_0 = -1/2(\Delta\sigma_T/\sigma)_{TOT}\ . \tag{21}$$

For $t < \frac{1}{2} t_1$, we have to a good approximation,

$$\begin{aligned} I(t) &\approx I_0\, e^{-t/t_0} \\ P(t) &\approx -t/t_1 \end{aligned} \tag{22}$$

Thus t_0 is the time scale associated with the attenuation of the $\bar{p}$ beam intensity, and t_1 is the time needed to build up an appreciable $\bar{p}$ polarization.

If t_1 is comparable to t_0, we have a chance to produce polarized $\bar{p}$'s before the beam disappears due to interactions with the target. However, in a realistic case, as shown in Table I, we have $\sigma_1/\sigma_0 < 0.1$ in the whole low energy region for models DR I, DR II, and PARIS. Thus $t_1 > 10\ t_0$, and the situation is unfavorable for producing appreciable polarization. The most favorable case we have found is model DR I at energies $E < 50$ MeV. Here σ_1/σ_0 is somewhat larger than the values listed in Table 1. For instance, for $E = 30$ MeV, an energy considered by Steffens[13], we find $\sigma_{TOT} = 272$ mb, $\sigma_1/\sigma_0 = 0.075$. Using the values[13] $n = 10^{14}/cm^2$, $f = 10^5/sec$, we find

$$\begin{aligned} t_0 &= 10.2 \text{ hrs} \\ t_1 &= 13.3\ t_0 = 136 \text{ hrs} \ . \end{aligned} \tag{23}$$

At $t = 48$ hrs, we then find

$$\begin{aligned} I(t) &= 0.0096\ I_0 \\ P(t) &= -\ 0.34 \ . \end{aligned} \tag{24}$$

The prospects for the success of the spin filtering technique[13] are thus rather grim. Even using the maximum value of σ_1/σ_0 predicted by

TABLE I.

Cross Section Ratio σ_1/σ_0 for Spin Filtering

E (MeV)	σ_1/σ_0 (PARIS)	σ_1/σ_0 (DR I)	σ_1/σ_0 (DR II)
70	0.055	0.052	0.030
100	0.062	0.044	0.017
130	0.065	0.037	0.009
160	0.065	0.032	0.003
190	0.063	0.028	0.002
220	0.061	0.025	-0.002
250	0.060	0.022	-0.003
280	0.058	0.020	-0.004
310	0.056	0.018	-0.006

our models, we still lose 99% of the beam before the $\bar{p}$ polarization has built up to values of about $-1/3$. The assumption that $\sigma_1/\sigma_0 \geq 0.1$, used by Steffens[13], is more optimistic than our realistic models suggest.

The spin observables of low and medium energy $N\bar{N}$ scattering represent a sensitive test of our theories of the meson exchange and annihilation potentials. A number of dramatic spin effects are anticipated, particularly in the $p\bar{p} \to n\bar{n}$ channel. A variety of models

which yield the same spin-averaged total cross sections lead to distinctively different spin dependences. The one pion exchange mechanism, supplemented by important contributions from vector meson exchanges, is crucial in producing marked spin dependences. Such effects are less important for total elastic and absorption cross sections. The coherent tensor potential due to π, ρ and ω exchanges dominates the spin physics of the $N\bar{N}$ system. Spin-orbit and spin-spin forces play a more modest role. The spin information to be gleaned from the $N\bar{N}$ system is somewhat complementary to that obtained from a study of NN scattering, where $\vec{L}\cdot\vec{S}$ and $\vec{\sigma}_1\cdot\vec{\sigma}_2$ terms play a more significant part. Spin data will be of premier importance in achieving a unified picture of the NN and $N\bar{N}$ interactions.

QUARK DYNAMICS OF $N\bar{N}$ ANNIHILATION: THE $\pi\rho$ PUZZLE

The annihilation modes of the $N\bar{N}$ system at low and medium energies enable us to probe aspects of the underlying quark-gluon dynamics which are not so clearly revealed in other processes. The signatures of quark dynamics appear in the form of approximate dynamical selection rules, that is, an unanticipated strong dependence of certain mesonic branching ratios on orbital angular momentum L, intrinsic spin S, and/or isospin I. The "standard" model describes $N\bar{N} \to$ mesons in terms of a baryon exchange mechanism. At high energies, where many L values contribute, this mechanism is well established[15]. It has been applied with some success to selected two meson $N\bar{N}$ annihilation modes by Moussallam[16]. For peripheral partial waves (large L), the idea of baryon exchange (i.e., three quarks with particular spin-flavor correlations and a well defined mass M and corresponding range 1/2M) seems reasonable, since the N and $\bar{N}$ quark "bags" do not overlap much in a collision with large impact parameter. For low partial waves (L=0,1), however, we expect the finite size of the N and $\bar{N}$ to play an important role. It is here that we hope to find evidence for quark-gluon degrees of freedom. For instance, baryon exchange models produce a smooth L dependence[14,16], while quark mechanisms can lead to a dramatic difference between L=0 and L=1 annihilation.

Let us illustrate these general remarks by consideration of a specific example, namely the annihilation mode

$$p\bar{p} \to \pi^+\pi^-\pi^0 \ . \tag{25}$$

An analysis of the old data with a liquid hydrogen target attributed 55% of the rate to the quasi-two-body (QTB) channel $\pi\rho$ and 45% to "incoherent" three-body $\pi^+\pi^-\pi^0$ events. The QTB channel πf was not seen (upper limit 10%). Because of the strong Stark effect in liquid, annihilation takes place mostly from L=0 (~93%, as per ref. (10)). A dynamical selection rule (DSR) on the branching ratios was observed, namely

$$BR(^{13}S_1 \to \pi^\pm\rho^\mp) \gg BR(^{31}S_0 \to \pi^\pm\rho^\mp) \tag{26a}$$

$$BR(^{31}S_0 \to (\pi^+\pi^-\pi^0)_{inc}) \gg BR(^{13}S_1 \to (\pi^+\pi^-\pi^0)_{inc}) \tag{26b}$$

where $^{2I+1,\ 2S+1}L_J$ labels the quantum numbers of the $N\bar{N}$ atom. By "dynamical," we mean that a transition permitted by general quantum

mechanical selection rules, such as $^{31}S_0 \to \pi^{\pm}\rho^{\mp}$, is suppressed.

Recent data from the ASTERIX collaboration[18] show a similar selection rule for L=1. With a gas target, they find that the reaction (25) consists of 40% $\pi\rho$, 40% $(\pi^+\pi^-\pi^0)_{inc}$ and 20% $\pi^0 f$. If we take into account the fact that $\bar{p}$ annihilation at rest in gas takes place about 57% of the time[19] from L=1 atomic orbits and 43% from L=0, we find for $p\bar{p} \to \pi^+\pi^-\pi^0$ the proportions

$$\begin{aligned} (\pi^+\pi^-\pi^0)^{I=1}_{inc} &= 0.36 \\ (\pi\rho)_{L=1} &= 0.29 \\ (\pi f)_{L=1} &= 0.35 \end{aligned} \tag{27}$$

A detailed analysis[18] yields

$$BR(^{11}P_1 \to \pi^{\pm}\rho^{\mp}) = 9 \cdot BR(^{33}P_{1,2} \to \pi^{\pm}\rho^{\mp}) \tag{28a}$$

$$BR(^{33}P_1 \to \pi^0 f) = 4 \cdot BR(^{33}P_2 \to \pi^0 f) \tag{28b}$$

Again, a transition allowed by general quantum mechanical selection rules ($^{33}P_{1,2} \to \pi^{\pm}\rho^{\mp}$) is not seen experimentally. We refer to the dynamical selection rules (DSR) of Eqs. (26) and (28) as the "$\pi\rho$ puzzle."

The explanation of DSR seems to require consideration of the quark-gluon mechanism of $p\bar{p}$ annihilation. The conventional baryon exchange mechanism[16] does not yield Eqs. (26) and (28) in any obvious way, although this question should be looked at in more detail. In the quark model, the relevant processes are depicted in Fig. 10. The pure rearrangement process R_3 can lead to the "incoherent" $\pi^+\pi^-\pi^0$ signal, which can also arise from the QTB processes R_2 and A_2, where one of the mesons is the very broad ε (an s-wave $\pi\pi$ enhancement with $J^{PC}(I^G) = 0^{++}(0^+)$). The other permissible QTB modes correspond to grouping $\pi^+\pi^-$ together to form the $\rho^\circ(1^{--}(1^+))$, $f(2^{++}(0^+))$, $g^\circ(3^{--}(1^+))$, etc., or taking $\pi^{\pm}\pi^0$ as a pair to make $\rho^{\pm}$, $g^{\pm}$, etc.

TABLE II.

Allowed Transitions[a] $p\bar{p} \to \pi^+\pi^-\pi^0$, considered as Quasi-two-body (QTB) Processes, for L=0,1

Initial State $^{2I+1,2S+1}L_J$	Final States
$^{31}S_0$	$\pi^0\varepsilon(\ell_f=0)$, $\pi^{\pm}\rho^{\mp}(\ell_f=1)$, $\pi^0 f(\ell_f=2)$
$^{13}S_1$	$\pi^0\rho^0$, $\pi^{\pm}\rho^{\mp}(\ell_f=1)$
$^{11}P_1$	$\pi^0\rho^0$, $\pi^{\pm}\rho^{\mp}(\ell_f=0,2)$
$^{33}P_1$	$\pi^0\varepsilon(\ell_f=1)$, $\pi^{\pm}\rho^{\mp}(\ell_f=0,2)$, $\pi^0 f(\ell_f=1,3)$
$^{33}P_2$	$\pi^{\pm}\rho^{\mp}(\ell_f=2)$, $\pi^0 f(\ell_f=1,3)$

[a] the relative orbital angular momentum of the two meson final state is denoted by ℓ_f

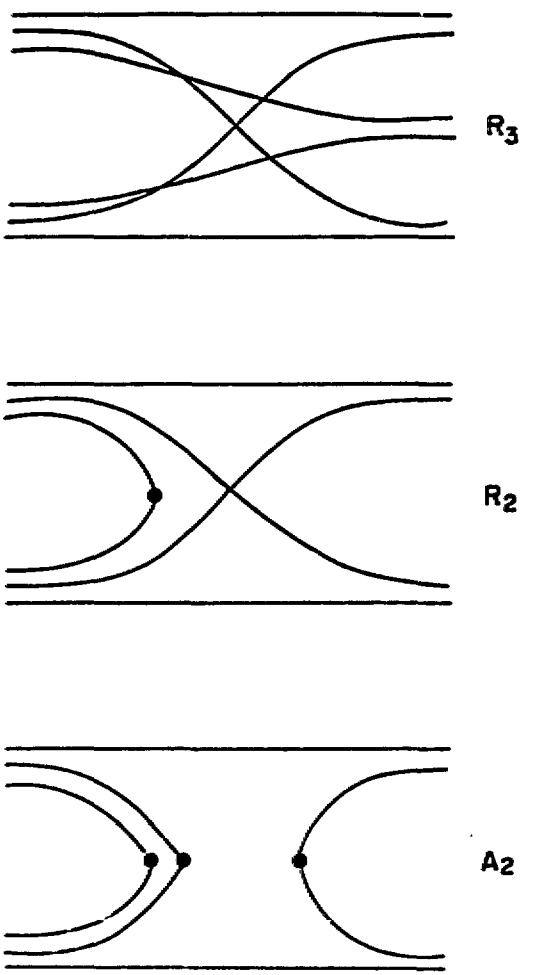

Fig. 10. Quark rearrangement and annihilation graphs for two (R_2,A_2) and three (R_3) meson final states from an initial $N\bar{N}$ system.

Since the πg mode offers very little phase space for production from $\bar{p}p$ at rest, we do not consider it further. The QTB transitions which are allowed by conservation of total angular momentum J, parity π, G-parity and C-parity (two neutral mesons only) are collected in Table II.

Now let us consider the selection rules associated with the quark graphs of Fig. 10. The rearrangement process R_3 is the simplest case. The effective operator is taken to be proportional to unity; that is, spin flip processes are assumed to be small, and hence $\Delta S = |S-S_f| = 0$ for the allowed transitions, where S is the $N\bar{N}$ intrinsic spin and S_f is the total intrinsic spin of the mesons. For R_3, if a unit of orbital angular momentum is pumped into the initial state, it reappears in the final state as an internal orbital angular momentum ℓ of the quark-antiquark ($Q\bar{Q}$) pair in a meson, not as a relative orbital angular momentum of two mesons. If $s = \{\pi,\eta,\eta',\rho,\omega\}$ denotes the family of s-wave mesons ($\ell=0$) and $p = \{\delta,\varepsilon,S^*,A_1,D,A_2,f,B,H\}$ the group of p-wave mesons ($\ell=1$), the selection rules for R_3 are

$$\begin{array}{lll} \text{Allowed transitions:} & L=0 \rightarrow sss \\ & L=1 \rightarrow ssp \\ \text{Forbidden transitions:} & L=0 \rightarrow ssp \\ & L=1 \rightarrow sss \end{array} \qquad (29)$$

The preferred transitions for R_2 and A_2 depend on the structure of the effective operator for $Q\bar{Q}$ annihilation (the dots in Fig. 10). Several authors[8,19] have used a one gluon vertex, of operator character $\vec{S}_{Q\bar{Q}} \cdot (\vec{\sigma}_i \times \vec{q})$, where $S_{Q\bar{Q}} = 1$ is the total $Q\bar{Q}$ intrinsic spin, $\vec{\sigma}_i/2$ is the spin of a second quark which is struck by the (dressed) gluon, and $\vec{q}$ is the momentum transferred to this quark. Some difficulties with this approach are discussed in ref. (10). Alternatively, one may assume[9,10] that the $Q\bar{Q}$ pair has the quantum numbers of the vacuum [$0^{++}(0^+)$, $^{13}P_0$ in LS coupling]. This choice is motivated by the success[20] of the "$^3P_0$ model" for meson and baryon resonance decays, in which only one $Q\bar{Q}$ pair is produced. The $^3P_0$ model can be "derived" in a strong coupling Hamiltonian lattice formulation[21] of QCD, in which gluons are replaced by flux tube degrees of freedom (collective modes of the gluon field). The "perturbative" and "strong coupling" versions of the effective $Q\bar{Q}$ vertex cannot be easily distinguished if one considers only total rates, i.e., spin averaged quantities. However, their distinct spin structures show up in the m-state populations of vector mesons produced from meson or $N\bar{N}$ atom decay. As noted in ref. (10), the polarization of (ρ,ω) in the decays $A_1 \rightarrow \pi\rho$ and $B \rightarrow \pi\omega$ is nicely consistent with the $^3P_0$ model, and at odds with the effective "one gluon" approach. We do not pursue this matter further here, and instead concentrate our attention on the $^3P_0$ model.

First let us consider $p\bar{p} \rightarrow \pi^+\pi^-\pi^0$ for L=0. The "incoherent" $\pi^+\pi^-\pi^0$ events can be understood as arising from graph R_3 or from $p\bar{p} \rightarrow \pi^0\varepsilon$, followed by the decay $\varepsilon \rightarrow \pi^+\pi^-$. Since $S_f=0$ for the three-body $\pi^+\pi^-\pi^0$ state, the $\Delta S=0$ selection rule for R_3 implies that $^{13}S_1 \rightarrow \pi^+\pi^-\pi^0$ is forbidden. From Table II, we further note that $^{13}S_1 \rightarrow \pi^0\varepsilon$ is forbidden (by J,π conservation and also by C conservation). Thus

we obtain immediately the selection rule (26b).

The $\Delta S=0$ selection rule is exact for graph R_3. For R_2 and A_2, the $\Delta S=0$ rule still holds approximately in the $^3P_0$ model, even though it is W-spin rather than ordinary intrinsic spin which is rigorously conserved, in analogy to the situation for meson and baryon resonance decays[20]. Thus we have

$$BR(^{13}S_1 \xrightarrow{\Delta S=0} \pi^{\pm}\rho^{\mp}) \gg BR(^{31}S_0 \xrightarrow{\Delta S=1} \pi^{\pm}\rho^{\mp}) , \tag{30}$$

providing an explanation of Eq. (26a). In any case, large production of $\pi\rho$ from the $^{13}S_1$ channel is expected, since from Table II we see that $\pi\rho$ is the only QTB channel permitted, whereas a $^{31}S_0$ state has in principle several decay options.

The absence of a $\pi^0 f$ signal for L=0 can also be understood if we note that $^{31}S_0 \to \pi^0 f(\ell_f=0)$ is forbidden by J conservation and $^{31}S_0 \to \pi^0 f(\ell_f=2)$ from A_2 or R_2 is suppressed.

Now consider $p\bar{p} \to \pi^+\pi^-\pi^0$ from an L=1 initial state. From Table II, we see that a sizable rate for $^{11}P_1 \to \pi\rho$ is anticipated, since only this mode is permitted (leading to $\pi^+\pi^-\pi^0$). On the other hand, the $^{33}P_1$ state can choose $\pi^0\varepsilon$, $\pi^{\pm}\rho^{\mp}$ or $\pi^0 f$ decay modes, each of which is a preferred $\Delta S=0$ transition. The competition between these modes depends on the relative amplitudes for processes R_2 and A_2. If we consider R_2 alone, we obtain

$$\begin{aligned} &BR(^{33}P_1 \to \pi^0\varepsilon,\ \pi^0 f) = 0 \\ &BR(^{33}P_1 \to \pi^{\pm}\rho^{\mp}) = 18 \cdot BR(^{11}P_1 \to \pi^{\pm}\rho^{\mp}) \end{aligned} \tag{31}$$

in complete contradiction to the data of Eqs. (27) and (28a). Estimates[22] indicate that R_2 and A_2 are comparable in amplitude; A_2 gives rise to substantial $\pi^0\varepsilon(\ell_f=1)$ and $\pi^0 f(\ell_f=1)$ production for L=1. We are thus able to understand the DSR of Eq. (28a) in terms of a depletion of $BR(^{33}P_{1,2} \to \pi^{\pm}\rho^{\mp})$ due to a severe competition from the $\pi^0\varepsilon$ and $\pi^0 f$ channels. The multi-channel aspect of the problem is thus seen to be crucial. One cannot just compare Born amplitudes for a single channel (i.e., $^{11}P_1 \to \pi^{\pm}\rho^{\mp}$ versus $^{33}P_1 \to \pi^{\pm}\rho^{\mp}$).

Given that $\pi^{\pm}\rho^{\mp}$ production is disfavored from the $^{33}P_1$ channel, and noting further that the transition $^{33}P_2 \to \pi^{\pm}\rho^{\mp}(\ell_f=2)$ is suppressed, we might naively expect that

$$BR(^{33}P_2 \to \pi^0 f) > \frac{5}{3} \cdot BR(^{33}P_1 \to \pi^0 f) \tag{32}$$

because of the statistical factor (2J+1) and the competition of the $\pi^0\varepsilon$ channel for $^{33}P_1$. This is in clear contradiction to Eq. (28b). However, this simple argument is incorrect because of the strong influence of isospin mixing: the very strong $N\bar{N}$ tensor potential induces a sizable mixing of $n\bar{n}$ and $p\bar{p}$ configurations[23], so that S=1 atomic states with L=0,1 are closer to being eigenstates of isospin than pure $p\bar{p}$ configurations. For instance, one finds that the $^3P_2$ atomic state is mostly I=0 at short distances (where annihilation takes place), the $^3P_1$ state is predominantly I=1, and the $^1P_1$ configuration has comparable I=0 and I=1 components (i.e., close to pure $p\bar{p}$). This mixing pattern arises because the tensor potential is coherently attractive for $^{13}P_2$, repulsive for $^{13}P_1$, and absent for

$^1P_1$. In the limiting case where the atomic eigenstates are taken to be $^{13}P_2$, $^{33}P_1$, and $1/\sqrt{2}(^{31}P_1 + {}^{11}P_1)$, we would assign statistical weights in the proportions $^{33}P_1 : {}^{11}P_1 : {}^{33}P_2 = 3:3/2:0$. This would explain the smallness of $\pi^0 f$ production from the $^{33}P_2$ channel, as in Eq. (28b).

For L=1, the "incoherent" $\pi^+\pi^-\pi^0$ production cannot come from graph R_3, because of the selection rule of Eq. (29), but rather from the transition $^{33}P_1 \to \pi^0\varepsilon$, followed by the decay $\varepsilon \to \pi^+\pi^-$. If we make the plausible assumption that $BR(^{33}P_1 \to \pi^0\varepsilon) \approx BR(^{33}P_1 \to \pi^0 f)$, since both are $\Delta S=0$, $\ell_f=1$ transitions, and use the modified statistical weights given above, then we expect

$$(\pi^+\pi^-\pi^0)^{L=1}_{inc} \approx (\pi^0\varepsilon)_{^{33}P_1} \approx 1/3 \qquad (33)$$

$$(\pi^0 f)_{^{33}P_1} \approx 1/3 \ , \quad (\pi\rho)_{^{11}P_1} \approx 1/3$$

in good agreement with the data of Eq. (27).

We have indicated how explicit consideration of the quark reaction amplitudes R_3, R_2 and A_2 of Fig. 10 can lead to an understanding of dynamical selection rules which have been observed in $\pi^+\pi^-\pi^0$ decays of L=0,1 $N\bar{N}$ atomic states. Similar considerations[10] lead one to an explanation of the observed strong suppression[24] of the K^+K^- and $K^0\bar{K}^0$ modes for L=1 relative to L=0. Such strange particle modes do not arise from R_3 or R_2, except due to the small strange quark admixtures in the initial state ($\Lambda\bar{\Lambda}$, $\Sigma\bar{\Sigma}$, etc.). Ratios such as $K\bar{K}/\pi\pi$ are thus a test of the relative size of R_2 and A_2. DSR are also expected in other annihilation channels such as 4π, 5π, $K\bar{K}\pi$, etc. Only the tip of the iceberg of DSR has been explored thus far! Precision measurements of relative branching ratios, as well as detailed amplitude analyses, are required. For these tasks, the premium is on $\bar{p}$ beams of high intensity. Other phenomena which are very revealing of the quark mechanism[10], and require high intensity beams, include i) ρ-ω interference, ii) ϕ production, and iii) polarization studies of vector mesons in annihilation.

THE FUTURE

We have emphasized only two aspects of the very rich area of low and medium energy $N\bar{N}$ interactions, namely spin observables and dynamical selection rules in $N\bar{N}$ annihilation. A substantial spin and isospin dependence is predicted for the $N\bar{N}$ interaction, but is not so readily revealed by elastic and annihilation cross sections alone. Measurements of spin observables are required, and these place a premium on obtaining the highest possible $\bar{p}$ beam intensities. Experiments with polarized beams and/or polarized targets are in general necessary to unravel the $N\bar{N}$ spin dependence, but much progress could already be made using a polarized target and an unpolarized $\bar{p}$ beam. Scattering of $\bar{p}$'s by nuclei and $p\bar{p}$ spin filtering do not seem promising as a means of producing polarized $\bar{p}$'s. The charge exchange process $p\bar{p} \to n\bar{n}$, on the other hand, leads to a highly polarized $\bar{n}$ beam.

The spin observables for the $N\bar{N}$ system provide a signature for the strong coherences in meson exchange forces (dominantly the tensor component) predicted by theory. NN and $N\bar{N}$ scattering are sensitive to somewhat complementary aspects of the same underlying interactions. The effects of coherent tensor forces are expected to be evident in $N\bar{N}$ spin quantities in spite of the strong influence of annihilation. Note that this tensor coherence is a feature which emerges from $\pi + \rho + \omega$ exchange, after the G-parity transformation has been applied to the NN potential. If one replaces the conventional vector mesons by an effective one gluon exchange mechanism, the strong tensor coherence does not survive (i.e., single gluon exchange, treated perturbatively, does not change sign like the ω in passing from NN to $N\bar{N}$). Thus if we wish to treat both the real and imaginary parts of the $N\bar{N}$ interaction on the same footing within the context of QCD, surely a laudable aim, the $N\bar{N}$ spin observables will exercise a strong constraint on the form of the effective operators.

The strong L dependence of certain $N\bar{N}$ annihilation modes and the existence of approximate selection rules offer promising signatures of the underlying quark-gluon dynamics. These selection rules highlight the difference between the decay of an ordinary $Q\bar{Q}$ meson and an $N\bar{N}$ system with the same external quantum numbers $\{L, S, J, I\}$. Even if one can understand these features in terms of a baryon exchange picture with phenomenologically adjusted coupling constants and vertices, a quark-gluon picture is likely to provide a more economical way of coming to grips with the observed selection rules and strong L dependence. High statistics experiments on $N\bar{N}$ annihilation are required in order to distinguish between models. Modes containing more than one neutral meson and rare modes involving ϕ production are also key elements in the picture. Once again, we find strong motivation for developing $\bar{p}$ beams of the highest possible intensity.

One area we have not addressed, but which was clearly one of the main motivating forces behind LEAR, is the use of the $N\bar{N}$ annihilation process to search for new mesons, such as baryonium states $(Q^2\bar{Q}^2)$, hybrids (QQg) or glueballs (gg, ggg). It now appears that such objects are unlikely to be long-lived, so their existence and quantum numbers can only be deduced by detailed amplitude analysis. Precise data on individual two-body annihilation channels, as a function of $\bar{N}$ energy, would be particularly valuable, since broad structures are notoriously difficult to extract from total cross sections. Such spectroscopy studies are underway at LEAR, but much work remains to be done.

In summary, there are numerous exciting physics questions which could be addressed with a dedicated low and medium energy $\bar{p}$ facility of even higher intensity than LEAR. Only a few of these have been discussed in this paper; many more are dealt with elsewhere in these Proceedings. It seems naive to assume that this area of physics will be so thoroughly mined by LEAR in the 1980s that little of interest will remain. A dedicated low energy $\bar{p}$ facility in the US should be given serious consideration.